

Long Distance Coupling of Lower Hybrid Waves in JET using Gas Feed

M Goniche¹, J A Dobbing, A Ekedahl², P Schild, F X Söldner.

JET Joint Undertaking, Abingdon, Oxfordshire, OX14 3EA,

¹Centre d'études de Cadarache, Association Euratom-CEA,
F-13108 Saint Paul-lez-Durance, France.

² Institute for Electromagnetic Field Theory and Plasma Physics,
Chalmers University of Technology. S-412 96 Göteborg, Sweden.

"This document is intended for publication in the open literature. It is made available on the understanding that it may not be further circulated and extracts may not be published prior to publication of the original, without the consent of the Publications Officer, JET Joint Undertaking, Abingdon, Oxon, OX14 3EA, UK".

"Enquiries about Copyright and reproduction should be addressed to the Publications Officer, JET Joint Undertaking, Abingdon, Oxon, OX14 3EA".

ABSTRACT.

Coupling experiments, using a gas feed near the Lower Hybrid Current Drive (LHCD) launcher, have been carried out in JET. An improvement in coupling for a given plasma - launcher distance can be obtained when the gas flow is large enough ($> 2.5 \times 10^{21}$ el./s). During these experiments, modification of the wall recycling was observed and the relation with the observed improvement in coupling is presented. For high gas flow ($> 5 \times 10^{21}$ el./s), a significant reduction in the suprathreshold electron population, as determined by non-thermal electron cyclotron emission and hard X-ray emission, is observed. Visible light imaging of a sector of the divertor indicates that some power might be coupled to the scrape-off layer when the injected gas flux is too high. At low gas flow, the coupling can be improved without affecting the LH power absorption in the plasma core.

1. INTRODUCTION

The Lower Hybrid Current Drive (LHCD) system in JET is mainly devoted to modifying the plasma current profile in order to access or improve high confinement regimes [1]. The launcher, which is powered by a 12 MW / 20 s generator at 3.70 GHz, is composed of twelve poloidally stacked rows (labelled 1 to 12 from top to bottom) of 32 narrow waveguides in the toroidal direction. In the launcher the radio frequency (RF) power is divided by E-plane multijunctions. Built-in phase shifters result in a 90° phasing between adjacent waveguides. This waveguide arrangement allows to launch a wave spectrum with a parallel index centred at $N_{//} = 1.8$, which is suitable for current drive [2].

Lower Hybrid (LH) waves can only propagate in a plasma with density above the cut-off density, n_{co} . More precisely, in order to have a good coupling of the LH waves to the plasma, the optimal electron density near the grill mouth must be in the order of

$$n_e = (N_{//}^2 - 1) \times n_{co}. \quad (1)$$

For the JET parameters this optimal edge density is $5 \times 10^{17} \text{ m}^{-3}$. This result is confirmed by the LH coupling code SWAN [3]. When the density in front of the launcher is close to this optimum, low reflection coefficient (2-5%) is obtained and high RF power can be coupled to the plasma. In these conditions, up to 7.3 MW has been coupled in JET. When there is departure from this optimum the electric field in the waveguides increases, which can lead to breakdowns and reduced power transmission capability. In the divertor configuration the e-folding decay length of the density in the scrape-off layer is small ($\lambda_n \sim 1-2 \text{ cm}$) and the launcher has to be approached close to the plasma. In most cases, the distance between the Last Closed Flux Surface (LCFS) and the launcher is only 1-3 cm. Feedback control of the launcher position on the average power reflection coefficient provides an efficient tool to maintain good coupling

when plasma conditions change [4]. However, in X-point plasma configurations with high triangularity, the plasma is shaped in such a way that there is a mismatch between the poloidal curvature of the launcher and that of the plasma. This mismatch, which is typically 2 cm, requires a trade-off for the optimal position and consequently some waveguide rows of the launcher are so close to the plasma that the excessive heat load on the tip of the waveguides may cause deleterious effects such as metallic impurity flux into the plasma.

In order to increase the operational range of the LHCD system, it is necessary to increase the distance at which good coupling can be obtained. In the 2.45 GHz LHCD experiments in ASDEX, it was first demonstrated that local gas injection could raise the electron density in the vicinity of the launcher and allow good coupling with an enlarged gap between the plasma and the launcher [5]. More recently, similar experiments were carried out in JT60-U, which has two LH launchers operated at 2 GHz. It was demonstrated that the distance between the antenna and the plasma could be increased up to 15-20 cm. The e-folding decay length of the density, as measured by a Langmuir probe, was unchanged when the gas was injected, but the density over the entire profile in the scrape-off layer was enhanced by almost a factor of 2 [6]. In ITER, due to technical constraints, a minimum gap of 15 cm between the LCFS and the launcher will be required. Because of the higher frequency proposed for ITER (5 GHz), this requirement is more demanding, since according to Eq. (1) the optimal density is increased by a factor of 6 with respect to the 2 GHz experiment. The coupling experiments carried out in JET is of particular interest for ITER, since the geometry of the JET tokamak is similar to the one of ITER and the operating frequency in JET is higher than in the experiments mentioned above.

This paper reports on experiments carried out in JET where gas was injected from a pipe near the launcher during LH pulses. Section 2 gives details on the gas injection system. The experimental procedure is given in Section 3. In Section 4, results showing the local modification of the edge plasma are presented, whereas the modification of the plasma-wall interaction is discussed in Section 5. Finally, experimental results showing a modification of the LH power absorption are presented in Section 6, before conclusions are drawn.

2. SET-UP OF GAS FEED

The main gas injection system in JET allows gas to flow from the divertor symmetrically around the torus. There are also additional pipes for localised gas feed. The so-called “near-grill” gas injection system used in the LH coupling experiments is composed of a pipe located in the outer wall, 1.3 m away from the launcher on the electron-drift side. The pipe has six holes, regularly spaced, see Fig. 1. For comparison, another gas feed, the so-called “far-grill” gas injection, which is located 8 m away from the launcher on the ion-drift side, was also used. Deuterium gas flow in the range $1-10 \times 10^{21}$ el./s at line average electron density $\bar{n}_e = 1.0-3.0 \times 10^{19} \text{ m}^{-3}$ was used in the experiments.

Experiments were performed with a safety factor, q_{95} , between 3.3 and 3.9. For this range of values, the holes of the near-grill gas injection are magnetically connected to the waveguide rows number 3 to 12 on the launcher. The gas pipe was later modified so that two holes were added at the upper part of the pipe, in order to have all twelve rows connected (Fig.1). For the far-grill gas injection, there is no magnetic connection between the launcher and the single gas injection point.

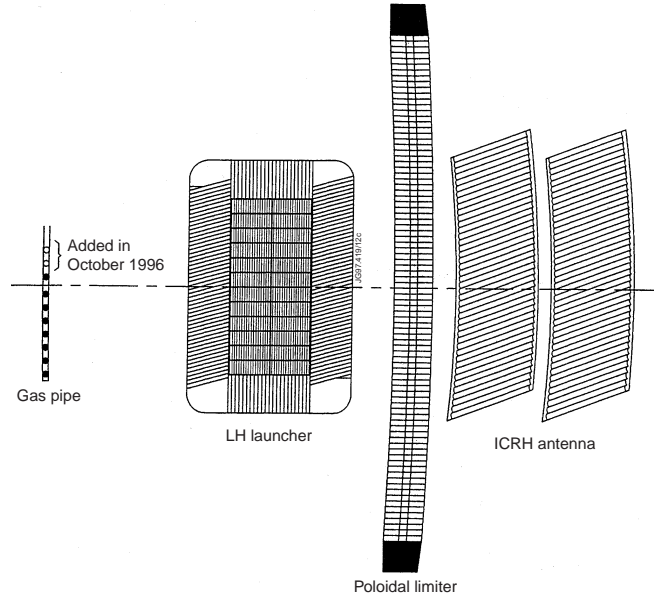


Fig.1. Drawing of the LHCD launcher environment. The near-grill gas pipe can be seen to the left of the launcher.

3. EXPERIMENTAL PROCEDURE

LHCD experiments with near-grill gas injection were carried out with LH power in the range 2-5 MW and with the standard 90° phasing between waveguides ($N_{||} = 1.8$). The main plasma parameters were the following: $B_T = 2.1-3.4$ T, $I_p = 1.0-2.5$ MA and $\bar{n}_e = 1.0-3.0 \times 10^{19} \text{ m}^{-3}$. The plasma was in the single-null divertor configuration. The radial position of the launcher and the LCFS were measured with reference to the position of the poloidal limiters. In all experiments, the plasma shape was such that the distance between the LCFS and the poloidal limiters was smaller above the mid-plane than below. At the level of row 1 of waveguides, this distance was only 2-3 cm, but increased to 4-5 cm in front of row 12. Generally, the plasma position was fixed during the LH pulse, but some results were obtained with the plasma moved away from the launcher.

For the launcher position, two types of operation were used. First the launcher was moved during the LH pulse with a pre-programmed waveform. Before the LH pulse the launcher was moved forward to the poloidal limiter radius ($r \approx 0$) or slightly in front of the limiters ($r \approx 1$ cm) and then moved backward to $r \approx -3.5$ cm. In the second case the position was feedback controlled on the average power reflection coefficient. In these experiments the set point value of the average reflection coefficient was 4%. When there was departure from this set point, the launcher moved with a speed depending on the amplitude of the error signal (Proportional-Integrator-Derivative feedback).

4. MODIFICATION OF LH COUPLING

By injecting gas near the launcher it is expected that the electron density can be increased locally and therefore good LH coupling can be obtained with a larger gap between the plasma and the antenna. In order to assess whether this effect is local, the same amount of gas was injected

from the near-grill and the far-grill injection system in consecutive pulses. Comparison between the near-grill gas feed and far-grill gas feed was established in two types of experiments, in order to verify that the result did not depend on the absolute launcher position and the mode of operation. First, the launcher was positioned 1 cm behind the poloidal limiters and the plasma moved away during the LH pulse. High gas flux, F , was used ($F = 8.5 \times 10^{21}$ el./s). A large difference in coupling was noticed for the two cases (Fig.2). In particular for the lower rows the reflection coefficient was maintained around 2% for a gap up to 9 cm for the near-grill gas feed case, whereas the reflection coefficient was larger than 10% when the gap exceeded 7 cm in the far-grill gas feed case. For the upper rows, a weaker effect of the near-grill gas injection was observed. In the second experiment, the plasma position was constant (3 cm away from the poloidal limiters) and the launcher position feedback controlled. The equilibrium position of the launcher for the same gas flux ($F = 1 \times 10^{22}$ el./s) was 2 cm behind the poloidal limiters for the near-grill gas feed case, whereas the launcher was slightly in front of the poloidal limiters in the far-grill gas feed case. The launcher position was similar in the far-grill case and a reference pulse, in which neither of the gas feeds was used.

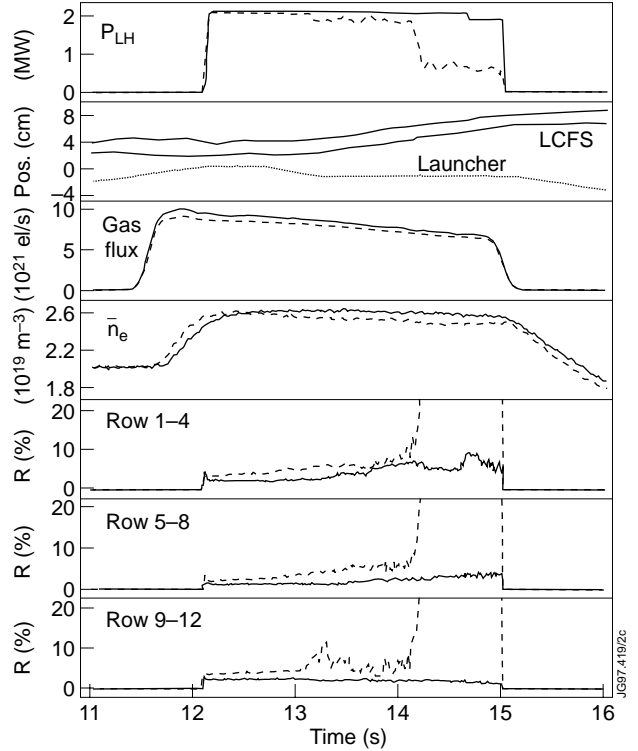


Fig.2. Effect of near-grill (solid lines, #37042) and far-grill (dashed lines, #37043) gas injection. LH power, launcher- and plasma positions, gas flux, line-averaged plasma density and reflection coefficients for rows 1-4, 5-8, 9-12 are shown.

This large improvement in coupling with the near-grill gas feed was obtained with high gas flux. For this case the line-averaged plasma density could not be maintained at the set point and increased from $2.0 \times 10^{19} \text{ m}^{-3}$ to $2.5 \times 10^{19} \text{ m}^{-3}$. Moreover, this high gas injection reduces drastically the LH power coupled to the bulk of the plasma. In order to optimise the near gas flux, the flow rate was varied from shot to shot from 0 to 5.5×10^{21} el./s. The gas flow was quasi-constant during the LH pulse. The launcher was moved from 0.5 cm ahead of the poloidal limiters to 3.5 cm behind the limiters. In this range of gas flow, large differences in the coupling were observed (Fig. 3). For the low gas feed case ($F = 2.3 \times 10^{21}$ el./s), the coupling was improved significantly for the lower rows. When the launcher was 2.5 cm behind the poloidal limiters, low reflection ($< 4\%$) was maintained on these rows. For the high gas feed case ($F = 5.5 \times 10^{21}$ el./s), further improvement was obtained and the launcher could be as far as 3.5 cm behind the poloidal limiters with good coupling for eight out of twelve waveguide rows. For the rows magnetically

connected to the gas injection pipe the reflection coefficient did decrease down to 2% regardless of the launcher position. This very good coupling with a large gap between the poloidal limiter and the launcher was also obtained with a lower gas flow ($F = 3.8 \times 10^{21}$ el./s).

After the modification of the gas pipe, which involved adding two more holes in the upper part of the pipe (Fig.1), further experiments were carried out. Especially, the gas feed was used for providing good coupling of the LH waves during the low density phase in the current ramp-up to the optimised shear discharges, where LHCD was utilised for current profile control. The evolution of the plasma parameters in such a discharge is shown in Fig.4. The launcher was retracted 7 mm behind the poloidal limiters throughout the LH pulse. Between 50% and 100% of the total gas flow required to sustain the main plasma density was supplied by the near-grill gas injection valve. Uniform coupling on all rows of the launcher was obtained when the gas flow was above the threshold value, i.e. $F \sim 2 \times 10^{21}$ el./s.

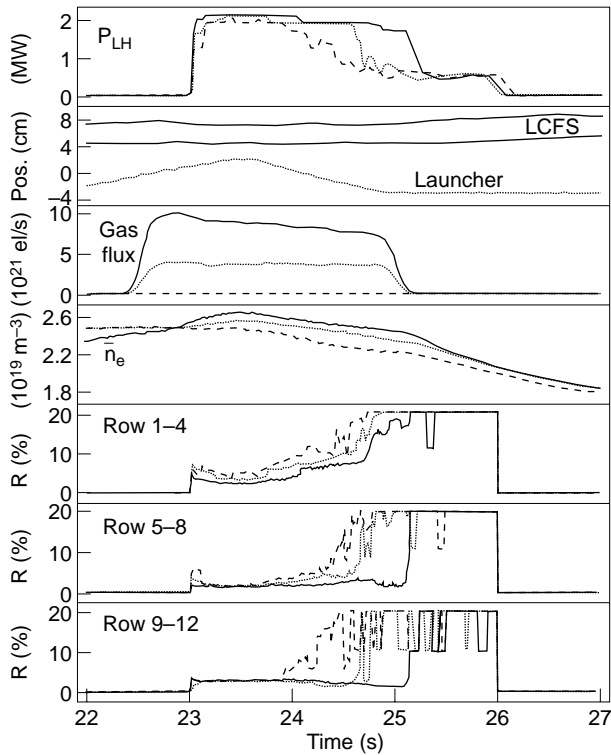


Fig.3. Effect of gas flux level. No gas (dashed lines, #36943), $F = 2 \times 10^{21}$ el./s (dotted lines, #36942) and $F = 6 \times 10^{21}$ el./s (solid lines, #36940). LH power, launcher and plasma positions, gas flux, line-averaged plasma density and reflection coefficients for rows 1-4, 5-8, 9-12 are shown.

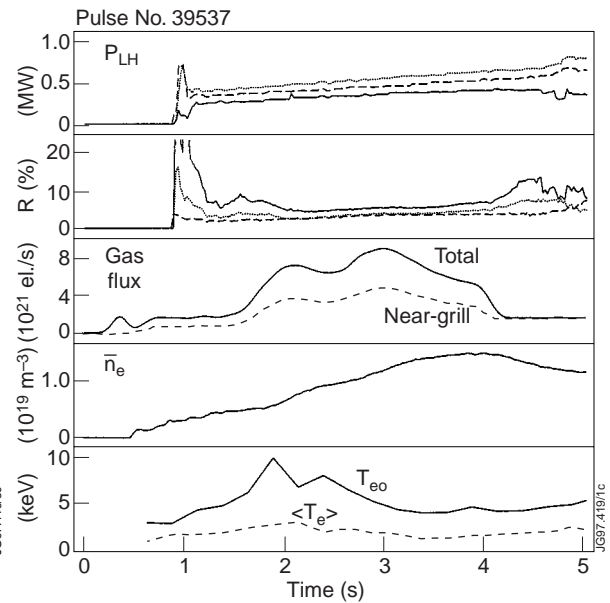


Fig.4. Coupling in the optimised shear experiments. The launcher is retracted 7 mm behind the poloidal limiters. The coupled power and reflection coefficient for waveguide rows 1-4 (solid lines), 5-8 (dotted lines) and 9-12 (dashed lines) are shown, together with gas flux, line average electron density and electron temperature.

5. MODIFICATION OF PLASMA-WALL INTERACTION

In the experiment with varying gas flow, described above, twelve shots were performed. First a pulse with no near-grill gas injection was carried out, then the gas flux was increased from shot

to shot and then progressively decreased again. Finally, the reference pulse with no gas from the near-grill gas valve was repeated. In order to compare the LH coupling properties for these shots, the maximum distance for which good coupling (i.e. reflection coefficient < 10%) could be achieved was recorded for the two upper rows, not connected to the gas feed pipe, and for the two lower rows, connected to the gas feed pipe. This distance is clearly not a univocal function of the gas flow level (Fig.5). After the high gas flux injection there was an improvement in coupling even with moderate gas flow ($F = 2-3 \times 10^{21}$ el./s), whereas before no effect on the coupling was observed at that same gas flow. For the ultimate pulse the near-grill gas feed was not used and good coupling was still obtained with a gap of 5-6 cm, which is a significant improvement with respect to the first reference pulse.

The density in front of the grill is clearly not dependent on the near-grill gas injection only. Recycling from the walls is likely to modify the edge density. D_α measurement from a CCD camera, located 3 m away from the launcher, monitors the recycling. For the first shots, the light emission remains low when LH is switched on (Fig. 6a), but when the gas flow is increased, the D_α signal increases with LH power (Fig. 6b). From pulse to pulse the wall behaviour is slightly modified by the gas injection and for the last pulse, in which the near-grill gas feed is not used, the recycling is still increased by ~ 40% with respect to the first reference pulse, consistent with the observed coupling improvement.

Once good coupling conditions were established with the near-grill gas feed, a delay of 200 ms between the closure of the valve and loss of coupling was found. The slow decay of the pressure in the pipe when the valve is closed is responsible for this delay (Fig.7). A rough estimate indicates that the gas flux was only reduced by 30% when the reflection coefficient jumped from 3% to 10%.

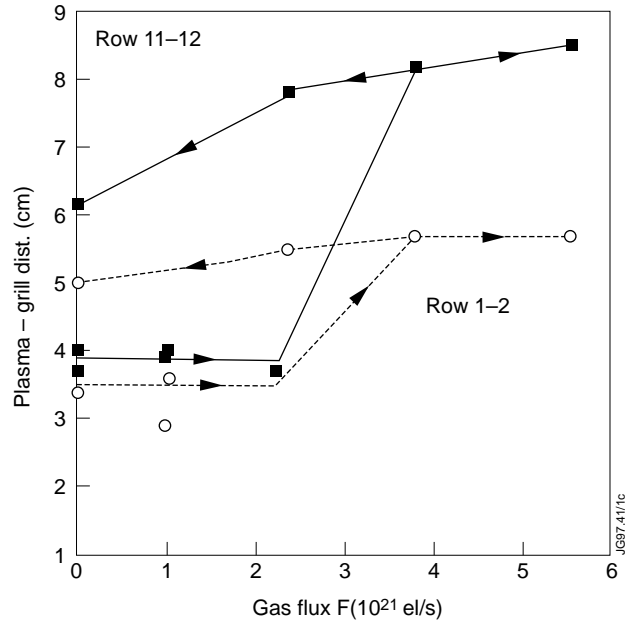


Fig.5. Maximum launcher-plasma distance for good coupling (reflection coefficient < 10%) versus near-grill gas flux for rows 1-2 (open circles) and rows 11-12 (filled squares).

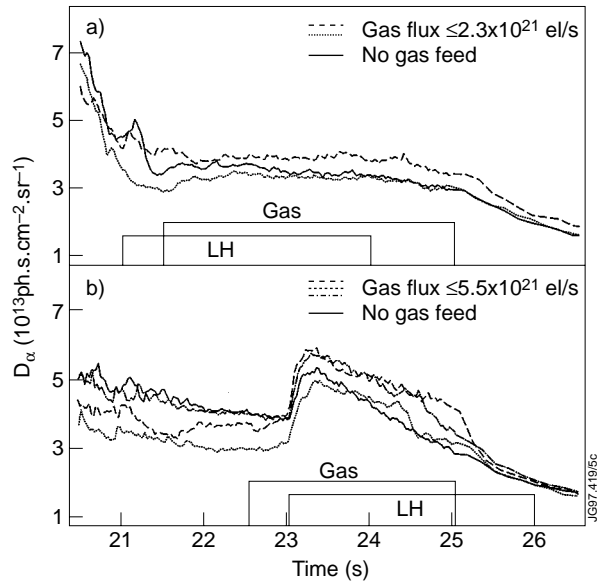


Fig.6. Evolution of D_α -signal from shot to shot.

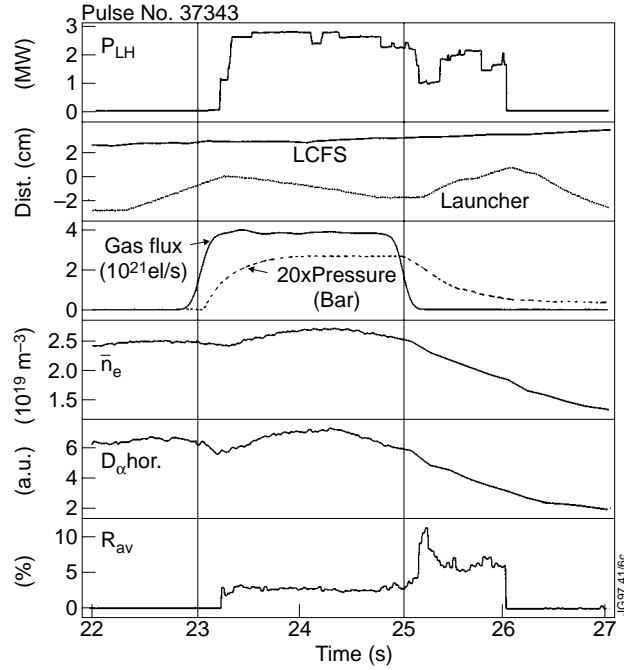


Fig.7. Near-grill gas feed with feedback control of the launcher position. Vertical dashed lines show when the gas valve is opened and closed. LH power, line-averaged plasma density, gas flux (solid line) and pressure in the pipe (dashed line), launcher- and plasma positions, average reflection coefficient and D_α are shown.

6. MODIFICATION OF LH POWER ABSORPTION

During the gas feed experiments the fast electron content of the discharge was monitored with both the Fast Electron Bremsstrahlung (FEB) diagnostic and the non-thermal component of the Electron Cyclotron Emission (ECE). The FEB diagnostic, which has nine vertical and ten horizontal channels, gives information about the LH power deposition profile [7]. The FEB emissivity has been compared in a reference case ($F = 0$) and a medium flux injection case ($F = 4.5 \times 10^{21}$ el./s). For the near-grill gas injection case, a decrease by almost a factor of two of the central chord signal is measured (Fig. 8). The same trend is observed for all horizontal chords of the diagnostic. There is no evidence that the LH power deposition profile is modified (Fig. 9). The non-thermal part of the ECE spectrum, coming from the downshifted

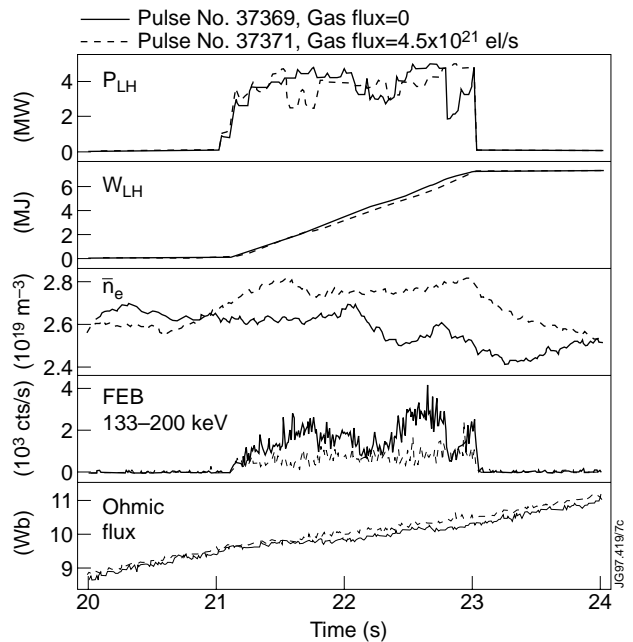


Fig.8. Effect of near-grill injection on plasma core signals. $F = 0$ (solid lines, #37369) and $F = 4.5 \times 10^{21}$ el./s (dashed lines, #37371). LH power, LH energy, line-averaged plasma density, FEB signal (central chord) and ohmic flux are shown.

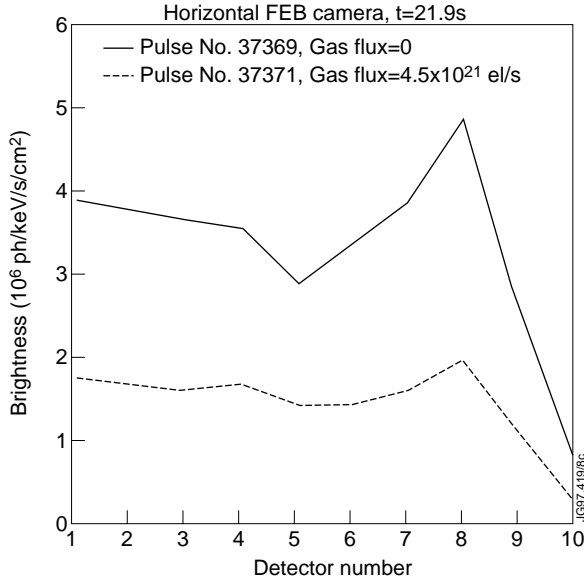


Fig.9. Effect of near-grill injection on FEB signals. $F = 0$ (solid line, #37369) and $F = 4.5 \times 10^{21}$ el./s (dashed line, #37371). Channel 6 views the centre of the plasma.

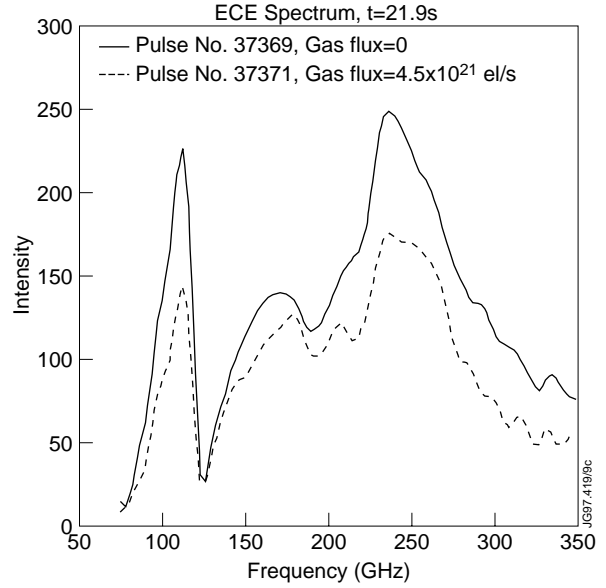


Fig.10. Effect of near-grill injection on ECE signals. $F = 0$ (solid line, #37369) and $F = 4.5 \times 10^{21}$ el./s (dashed line, #37371). The second harmonic downshifted emission (non-thermal contribution) is located at around 110 GHz.

second harmonic emission ($f \approx 110$ GHz) is reduced by $\sim 35\%$ (Fig. 10). In these two 2.5 MA discharges at relatively high density ($\bar{n}_e = 2.7 \times 10^{19} \text{ m}^{-3}$), half of the current is driven by the LH waves. It is estimated from the measurement of the magnetic flux consumption that the current drive efficiency is reduced by $15 \pm 15\%$. The line integrated FEB emission from the ten horizontal channels, integrated over the whole LH pulse and corrected for the slightly different density (less than 5%), lead to a loss of fast electrons of $45 \pm 10\%$. However, analysis of further LH discharges, performed during the current ramp-up phase, indicates that the drop in current drive efficiency may be in the order of 30% when gas flow $F > 4 \times 10^{21}$ el./s is used.

As the gas flow increases, the FEB signal normalised to reference pulses without gas feed, decreases (Fig. 11). However, close to the threshold where improvement in the coupling is obtained ($F = 2\text{-}3 \times 10^{21}$ el./s), the reduction in the fast electron content and the decrease in current drive efficiency is small ($< 15\%$). Generally speaking, there is a correlation between the improvement in coupling and the loss of power absorbed in the plasma, as derived from FEB and

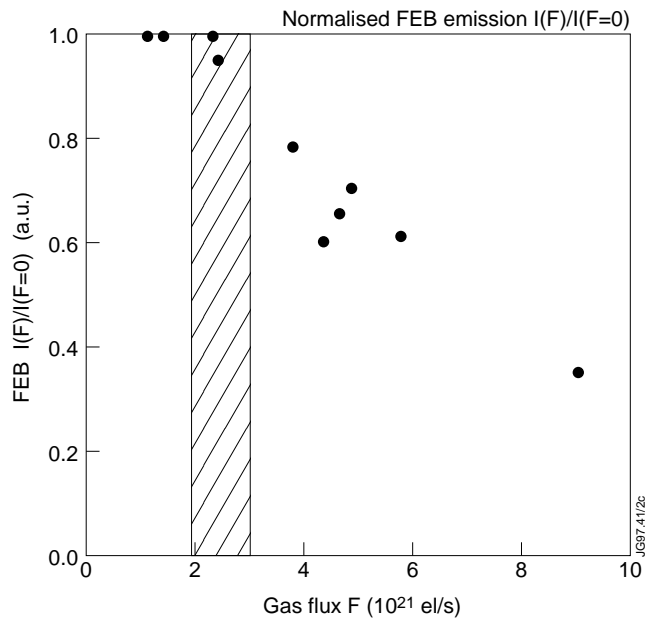


Fig.11. Normalised FEB emission, $I(F)/I(F=0)$, versus gas flux, F .

ECE measurements. This is supported by different observations. Firstly, with the far-grill gas feed, no significant loss of fast electrons is observed. Secondly, pulses performed after heavy gas injection experiments show a reduction in fast electron content, compared with earlier pulses at the same gas feed.

The power which is lost from the bulk of the plasma is likely be coupled to the scrape-off layer. Direct ionisation of the gas by the LH power is a possible mechanism that can explain the improvement in coupling. A rough estimate of the minimum power required in order to produce a layer of plasma with thickness e_p and density n_e in front of the launcher can be given by the following considerations. If E_i is the ionisation potential of the gas, the required energy is

$$E = n_e e_p L_{//} L_p E_i,$$

where $L_{//}$ and L_p are the toroidal and poloidal extents of the launcher, respectively. This energy must be renewed at every confinement time of the particles. If no collisions are taken into account, the confinement time is simply the transit time of the particles in front of the grill, i.e.

$$\tau = L_{//} / v_{th},$$

where v_{th} is the velocity of the electrons in the scrape-off layer. The minimum power needed to sustain this plasma is therefore

$$P_{min} = E / \tau = n_e v_{th} e_p L_p E_i.$$

The ionisation potential of the hydrogen molecule is 15.4 eV and if radiation losses are taken into account, the effective ionisation energy is 4-5 times larger. With $n_e = 5 \times 10^{17} \text{ m}^{-3}$, $T_e = 15 \text{ eV}$, $e_p = 0.03 \text{ m}$, $L_p = 1 \text{ m}$ and $E_i = 70 \text{ eV}$, we get

$$P_{min} \approx 350 \text{ kW}.$$

It has to be pointed out that, with the above plasma edge parameters, the mean free path of the electrons is much larger than the grill dimensions and the loss mechanism, i.e. recombination, should not be dominant. In order to sustain such a plasma, the absorbed power should not exceed 10-15% of the injected power, which was 2-5 MW in these experiments. Therefore, another mechanism seems necessary in order to explain the high level of power absorbed in the scrape-off layer at high gas flow.

In both TdeV [8] and Tore Supra [9], localised power deposition on components magnetically connected to the launcher has been observed in LHCD experiments. In JET, for the range of safety factors in these experiments ($q_{95} = 3.3-3.9$), calculations of the field line trajectories show that on the electron-drift side the launcher is connected either to the divertor plates or to a poloidal limiter. The strike point for the same plasma configuration depends on the launcher position. When the launcher is in front of the poloidal limiters, it is connected to the outer target

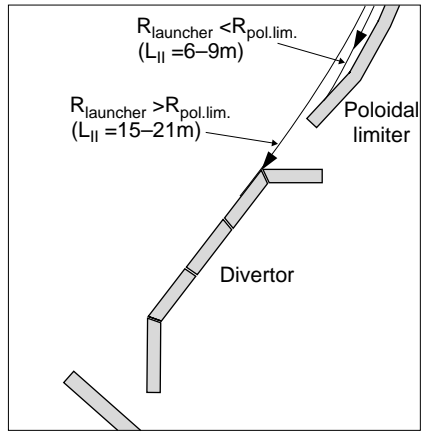
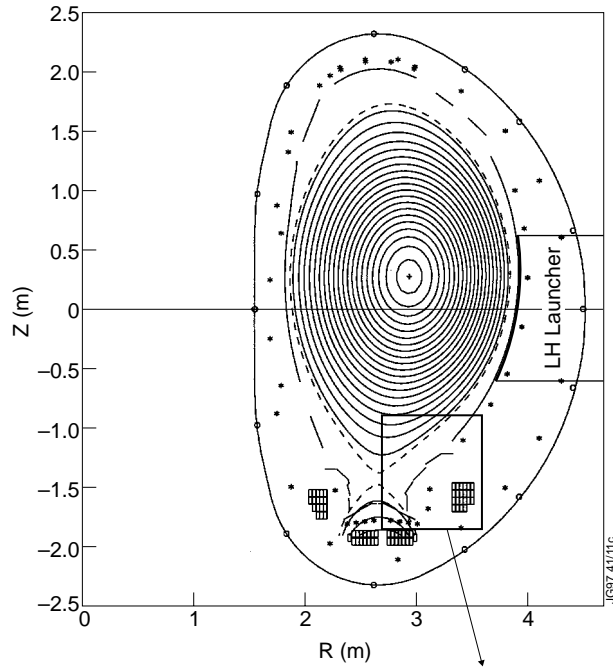


Fig.12. Poloidal section of JET plasma showing field line connections between the launcher and the divertor or the poloidal limiter.

plates of the divertor and the connection length is $L_{||} = 15-21$ m, see Fig. 12. When the launcher is slightly behind the poloidal limiters, the field line from the launcher strikes the bottom of one of the two poloidal limiters, denoted 5RH and 6LH (Fig. 13), or the horizontal divertor plates just below these limiters. In this case the connection length is $L_{||} = 6-9$ m (Fig. 12). A CCD camera views this section of the torus and the recycling can be monitored. When comparing two pulses, for which the launcher was almost flush with the poloidal limiter and the injected power was 3.5 MW, light can be seen on hori-

zontal plates of the divertor and on the very bottom of the 5RH poloidal limiter when the near-grill gas feed is used (Fig. 14b). These components remain dark when the gas feed is not used (Fig. 14a). For these pulses, the gas flux was low ($F = 2.5 \times 10^{21}$ e.l./s) and the coupling was only slightly improved. In a pulse with higher gas flux ($F = 5.3 \times 10^{21}$ e.l./s), the launcher was moved from flush with the poloidal limiters to 2 cm behind the limiters during the pulse. Despite the lower LH power (2.5 MW), the emission is strongly enhanced with respect of the low gas feed case for the same launcher position. When the launcher is flush, light emission can be seen on all the horizontal tiles between 5RH and 6RH (Fig. 15a). When the launcher is 2 cm behind the poloidal limiters, the light emissivity of these tiles is further enhanced (Fig. 15b). The field line trajectory calculation shows that when the launcher is

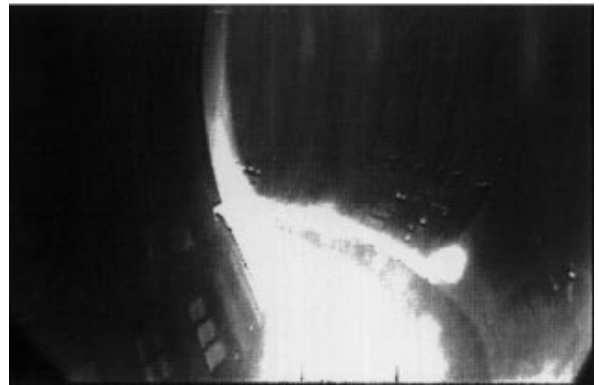
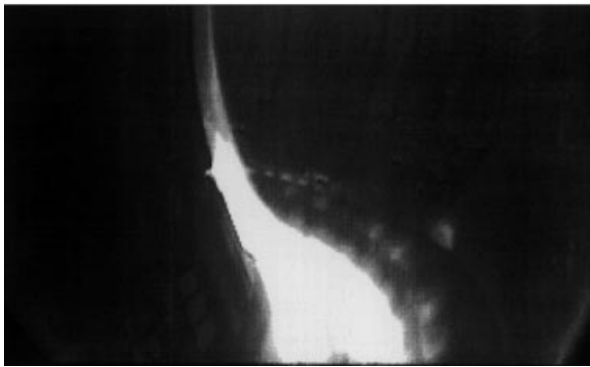
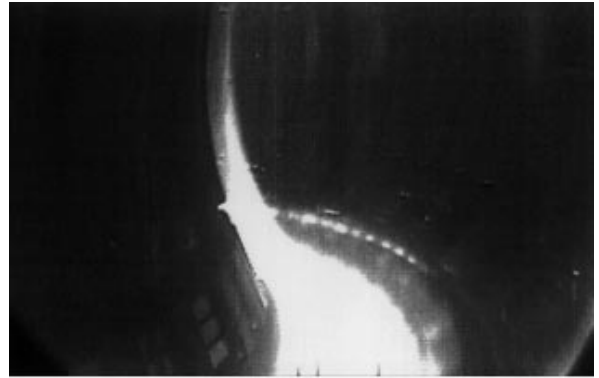


Fig.14. CCD images for $R_{launcher} - R_{pol.lim} = 0$ and $P_{LH} = 3.5$ MW. (a) $F = 0$, (b) $F = 2.5 \times 10^{21}$ el./s.

Fig.15. CCD images for $F = 5.3 \times 10^{21}$ el./s and $P_{LH} = 2.5$ MW. (a) $R_{launcher} - R_{pol.lim.} = 0$, (b) $R_{launcher} - R_{pol.lim.} = 2$ cm.

flush with the limiters it is mainly connected to the divertor target plates and only two or three rows are connected to the viewed section, whereas when the launcher is 2 cm behind, all the rows below the mid-plane are connected either to the horizontal plates or the 5RH limiter.

As reported in Section 5, the improvement in coupling is lost ~ 200 ms after the gas valve is closed, indicating that the enhanced edge density is not sustained by the RF power when the particle source is reduced. Consistently, the CCD images indicate that the localised recycling on launcher-connected areas decays very rapidly when the gas feed is stopped. When the LH power is switched off, the emissivity decays within the camera frame time repetition rate (40 ms). This indicates that the thermal contribution to the emissivity in the visible range is negligible and therefore the temperature of the tiles stays below 500°C .

7. CONCLUSIONS

In order to increase the distance between the launcher and the LCFS, the gas feed near the grill is effective and good coupling of high LH power can be obtained with the launcher as far as 3.5 cm behind the poloidal limiters. In this case, the connection length of the magnetic field lines passing in front of the launcher is only 2.5 m and, because of the short e-folding decay length of

the density ($\lambda_n < 1$ cm), the local electron density has to be strongly enhanced by a RF-induced effect to explain the good coupling.

Despite the larger plasma-launcher distance for the lower rows compared to the upper rows, the coupling is more substantially improved on the lower rows. The experimental set-up allows these rows to be magnetically connected to the gas feed holes. The gas pipe has now been modified in order to have all twelve rows connected to the holes and to improve the coupling more uniformly.

The gas flow has to be optimised to avoid a reduction of the power absorbed in the plasma core. Since the coupling distance also depends on the intrinsic particles source, namely the recycling, a feedback control of the near-grill gas flux on the LH coupling will improve the efficiency. Such a feedback system has now been implemented on JET.

The fraction of power absorbed in the scrape-off layer at high gas flow (> 20%) suggests that another mechanism, rather than simple ionisation in front of the grill, may occur. On TdeV, similar losses are observed when the density in front of the grill is high. A model of acceleration in the near-field of the antenna by the very high $N_{//}$ components of the spectrum leads to a rather good prediction of the experimental results.

Visible imaging of plasma-facing components magnetically connected to the launcher indicates a significant increase of recycling, suggesting a localised heat flux when the near-grill gas flow is high. Quantitative measurements on these components, like infrared imaging or thermometry, during long LH pulses should assess the fraction of LH power coupled to the scrape-off layer, and whether this is in accordance with the measurements of the power lost from the bulk plasma, as deduced from FEB, ECE and magnetic data.

During these experiments with large distance between the plasma and the launcher, very low metallic impurity flux was recorded from spectroscopic measurements. Local gas injection therefore provides good coupling with the launcher in a safe position behind protective limiters.

ACKNOWLEDGMENTS

The authors are grateful to the LHCD group and the JET staff involved for their support in carrying out these experiments.

REFERENCES

- [1] F.G. Rimini, et al., Proc. 11th Top. Conf. on RF Power in plasmas, Palm Springs, California, USA, 1995, pp. 110-113.
- [2] M. Pain, et al., Proc. 13th Symposium on Fusion Engineering, Knoxville, Tennessee, USA, 1989.
- [3] X. Litaudon and D. Moreau, Nuclear Fusion **30** (1990) 471.

- [4] M. Lennholm, et al., Proc. 16th Symposium on Fusion Engineering, Urbana-Champaign, Illinois, USA, 1995.
- [5] F. Leuterer, et al., Plasma Physics and Controlled Fusion **33** (1991) 169.
- [6] H. Kimura, et al., Proc. 11th Top. Conf. on RF Power in Plasmas, Palm Springs, California, USA, 1995, pp. 81-89.
- [7] P. Froissard et al., Proc. 18th EPS Conf. on Controlled Fusion and Plasma Physics, Berlin, FRG, 1991, Vol. 15, Part III, pp. 389-392.
- [8] J. Mailloux, et al., to be published in Jour. Nucl. Mater. (1997).
- [9] M. Goniche, et al., Proc. 23rd EPS Conf. on Controlled Fusion and Plasma Physics, Kiev, Ukraine, 1996, Vol. 20C, Part II, pp. 783-786.